

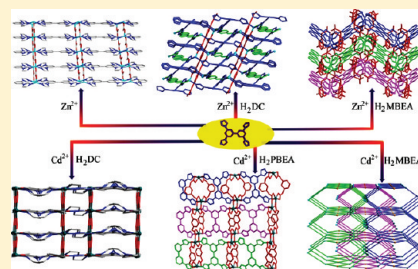
# Zinc(II) and Cadmium(II) Complexes with Rigid 3,3',5,5'-Tetra(1H-imidazol-1-yl)-1,1'-biphenyl and Varied Carboxylate Ligands

Li Luo, Peng Wang, Guan-Cheng Xu, Qing Liu, Kai Chen, Yi Lu, Yue Zhao, and Wei-Yin Sun\*

Coordination Chemistry Institute, State Key Laboratory of Coordination Chemistry, School of Chemistry and Chemical Engineering, Nanjing National Laboratory of Microstructures, Nanjing University, Nanjing 210093, China

## S Supporting Information

**ABSTRACT:** Six new coordination polymers  $[\text{Zn}(\text{L})_{0.5}(\text{CO}_3)] \cdot \text{H}_2\text{O}$  (**1**),  $[\text{Zn}(\text{L})_{0.5}(\text{DC})] \cdot \text{H}_2\text{O}$  (**2**),  $[\text{Cd}(\text{L})_{0.5}(\text{DC})]$  (**3**),  $[\text{Cd}(\text{L})_{0.5}(\text{PBEA})] \cdot \text{H}_2\text{O}$  (**4**),  $[\text{Cd}_2(\text{L})(\text{MBEA})_2] \cdot 4\text{H}_2\text{O}$  (**5**), and  $[\text{Zn}(\text{L})_{0.5}(\text{MBEA})] \cdot 2\text{H}_2\text{O}$  (**6**) with different structures and topologies were successfully synthesized by hydrothermal reactions of zinc(II)/cadmium(II) salts with rigid ligand 3,3',5,5'-tetra(1H-imidazol-1-yl)-1,1'-biphenyl (**L**) and auxiliary multicarboxylic acids of 1,3,5-tri(4-carboxyphenyl)benzene ( $\text{H}_3\text{BTB}$ ), 1,4-benzenediacrylic acid ( $\text{H}_2\text{DC}$ ), 1,4-benzenediacetic acid ( $\text{H}_2\text{PBEA}$ ), and 1,3-benzenediacetic acid ( $\text{H}_2\text{MBEA}$ ), respectively. Carbonate anion, rather than the carboxylate anion of  $\text{H}_3\text{BTB}$ , is incorporated in **1**. Complexes **1** and **5** are (4,4)- and (4,6)-connected binodal two-dimensional (2D) networks with a point (Schläfli) symbol of  $(4.6^4.8)_2(4^2.6^4)$  and  $(3^2.4^2.5^2)(3^4.4^4.5^4.6^3)$ , respectively. Complex **2** is a self-penetrating three-dimensional (3D) framework with a point (Schläfli) symbol of  $(6^2.8^4)(6^4.8^2)_2$ , while **3** shows a (3,4,5)-connected trinodal 3D framework with a point (Schläfli) symbol of  $(4.6^3.8^6)_2(4^2.8^4)(6^3)_2$ . The 3-fold interpenetrating net of **4** is a subnet of **sta** with a point (Schläfli) symbol of  $(4.6^4.8)_2(4^2.6^2.8^2)$ , while the net of **6** is vested in **nbo** set net with a point (Schläfli) symbol of  $(6^4)(8^2)$ . The results show that the auxiliary ligands and metal centers play important roles in the formation of complexes with diverse structures. Furthermore, the thermal stability, photoluminescence, and sorption properties of the complexes were investigated.



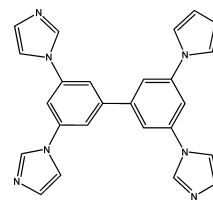
## INTRODUCTION

The construction of coordination polymers with novel structures and topologies has attracted great attention of chemists not only owing to their undisputed array of structures such as bowl, cage, helix, self-penetrating/interpenetrating frameworks, etc., but also because of their potential applications in gas storage/separation, optics, and so on.<sup>1–8</sup> According to the previously reported studies, tetradentate ligand with nitrogen donors, for example, 1,2,4,5-tetrakis(imidazol-1-ylmethyl)benzene, 4,4',6,6'-tetrakis(4-pyridyl)bimesityl, and 3,3',5,5'-tetrakis(3-pyridyl)-1,1'-biphenyl have been demonstrated to be powerful building blocks in the assembly of metal–organic frameworks (MOFs) with novel structures and topologies of corundum, diamond, PtS, etc.<sup>9–11</sup> On the other hand, many outstanding research studies have been carried out using carboxylate ligands such as terephthalic acid, 1,3,5-benzenetricarboxylic acid, 1,4-benzenediacrylic acid, 1,4-benzenediacetic acid, and 1,3-benzenediacetic acid to build MOFs with diverse structures and interesting properties.<sup>12–16</sup> Moreover, the carboxylate ligands have enriched coordination modes. On the basis of the advantage of nitrogen donor and carboxylate ligands, the strategy using mixed carboxylate and nitrogen donor ligands has come into play in the construction of MOFs.<sup>17–19</sup> Until now, much research based on mixed imidazole-containing ligand and multicarboxylate has been carried out. In our previous studies, we adopted 1,4-di(1H-imidazol-4-yl)benzene, 1,3,5-tris(1-imidazolyl)benzene, and 1,2,4,5-tetrakis(imidazol-1-ylmethyl)benzene

combined with multicarboxylate ligands and successfully obtained complexes with diverse structures and topologies as well as specific properties.<sup>2d,9c,18</sup>

As a continuation of our previous works, a new rigid tetradentate ligand 3,3',5,5'-tetra(1H-imidazol-1-yl)-1,1'-biphenyl (**L**, Scheme 1) was designed, which has more coordination

## Scheme 1. Schematic Drawing for the Ligand L



sites and conjugated aromatic groups. We used the combination of **L** with 1,3,5-tri(4-carboxyphenyl)benzene ( $\text{H}_3\text{BTB}$ ), 1,4-benzenediacrylic acid ( $\text{H}_2\text{DC}$ ), 1,4-benzenediacetic acid ( $\text{H}_2\text{PBEA}$ ), 1,3-benzenediacetic acid ( $\text{H}_2\text{MBEA}$ ), and  $\text{Zn}^{\text{II}}/\text{Cd}^{\text{II}}$  salts to construct novel coordination polymers. We here intend to compare the diversities of the structures by changing the

Received: February 15, 2012

Revised: March 30, 2012

Published: April 2, 2012

structure and flexibility of the carboxylate ligands under similar experimental conditions. Herein, we report the syntheses, crystal structures, and properties of six new Zn<sup>II</sup>/Cd<sup>II</sup> coordination polymers, namely, [Zn(L)<sub>0.5</sub>(CO<sub>3</sub>)]·H<sub>2</sub>O (**1**), [Zn(L)<sub>0.5</sub>(DC)]·H<sub>2</sub>O (**2**), [Cd(L)<sub>0.5</sub>(DC)] (**3**), [Cd(L)<sub>0.5</sub>(PBEA)]·H<sub>2</sub>O (**4**), [Cd<sub>2</sub>(L)(MBEA)<sub>2</sub>]·4H<sub>2</sub>O (**5**), [Zn(L)<sub>0.5</sub>(MBEA)]·2H<sub>2</sub>O (**6**).

## EXPERIMENTAL SECTION

All commercially available chemicals and solvents are of reagent grade and were used as received without further purification. Elemental analyses for C, H, and N were performed on a Perkin-Elmer 240C elemental analyzer at the analysis center of Nanjing University. Thermogravimetric analyses (TGA) were performed on a simultaneous SDT 2960 thermal analyzer under nitrogen with a heating rate of 10 °C min<sup>-1</sup>. Fourier transform infrared (FT-IR) spectra were recorded in the range of 400–4000 cm<sup>-1</sup> on a Bruker Vector22 FT-IR spectrophotometer using KBr pellets. Powder X-ray diffraction (PXRD) patterns were obtained on a Shimadzu XRD-6000 X-ray diffractometer with Cu Kα (λ = 1.5418 Å) radiation at room temperature. The luminescence spectra for the powdered solid samples were measured on an Aminco Bowman Series 2 spectrofluorometer with a xenon arc lamp as the light source. In the measurements of emission and excitation spectra, the pass width is 5 nm, and all the measurements were carried out under the same experimental conditions. Sorption experiments were carried out on a Belsorp-max volumetric gas sorption instrument. The bulk samples of **1** and **6** for sorption experiments were obtained by heating the fresh complexes at 190 and 180 °C, respectively, for 10 h under high vacuum to remove the free water molecules.

**Synthesis of Ligand L.** The compound L was prepared in 75% yield by using 3,3',5,5'-tetrabromo-1,1'-biphenyl (5.64 g, 12.0 mmol),<sup>20</sup> imidazole (6.54 g, 96.0 mmol), K<sub>2</sub>CO<sub>3</sub> (8.84 g, 64.0 mmol), and anhydrous CuSO<sub>4</sub> (64.0 mg, 0.40 mmol) following the previously reported procedures used for synthesis of 1,3,5-tris(7-azaindol-1-yl)-benzene.<sup>21</sup> <sup>1</sup>HNMR [(CD<sub>3</sub>)<sub>2</sub>SO]: δ = 8.58 (s, 4H), 8.16 (s, 4H), 8.07 (s, 6H), 7.20 ppm (s, 4H). Anal. Calcd for C<sub>24</sub>H<sub>18</sub>N<sub>8</sub>: C, 68.89; H, 4.34; N, 26.78%. Found: C, 68.72; H, 4.22; N, 26.69%.

**Preparation of [Zn(L)<sub>0.5</sub>(CO<sub>3</sub>)]·H<sub>2</sub>O (**1**).** A mixture of L (10.5 mg, 0.025 mmol), ZnSO<sub>4</sub>·7H<sub>2</sub>O (14.4 mg, 0.05 mmol), H<sub>3</sub>BTB (13.1 mg, 0.03 mmol), and NaHCO<sub>3</sub> (8.4 mg, 0.1 mmol) in 8 mL of H<sub>2</sub>O was sealed into Teflon-lined stainless steel container and heated at 180 °C for 3 days. After the mixture was cooled to room temperature, yellow block crystals were obtained in 65% yield. Anal. Calcd for C<sub>13</sub>H<sub>11</sub>N<sub>4</sub>O<sub>4</sub>Zn: C, 44.28; H, 3.14; N, 15.89%. Found: C, 44.17; H, 3.06; N, 15.84%. IR (KBr pellet, cm<sup>-1</sup>): 1618 (s), 1520 (s), 1483 (s), 1401 (s), 1244 (m), 1112 (m), 1067 (s), 966 (w), 876 (w), 845 (m), 758 (m).

**Preparation of [Zn(L)<sub>0.5</sub>(DC)]·H<sub>2</sub>O (**2**).** A mixture of (10.5 mg, 0.025 mmol), ZnSO<sub>4</sub>·7H<sub>2</sub>O (14.4 mg, 0.05 mmol), H<sub>2</sub>DC (10.9 mg, 0.05 mmol), and NaOH (4.0 mg, 0.1 mmol) in 8 mL of H<sub>2</sub>O was sealed into Teflon-lined stainless steel container and heated at 180 °C for 3 days. After the mixture was cooled to room temperature, yellow crystals of **2** were obtained in 85% yield. Anal. Calcd for C<sub>24</sub>H<sub>19</sub>N<sub>4</sub>O<sub>5</sub>Zn: C, 56.65; H, 3.76; N, 11.01%. Found: C, 56.50; H, 3.69; N, 10.96%. IR (KBr pellet, cm<sup>-1</sup>): 1641 (s), 1600(s), 1513 (m), 1354 (s), 1245 (w), 1120 (w), 1072 (m), 970(w), 946 (w), 854 (w), 756 (w).

**Preparation of [Cd(L)<sub>0.5</sub>(DC)] (**3**).** Complex **3** was obtained by the same procedure used for preparation of **2** except that ZnSO<sub>4</sub>·7H<sub>2</sub>O (14.4 mg, 0.05 mmol) was replaced by CdSO<sub>4</sub>·8/3H<sub>2</sub>O (12.9 mg, 0.05 mmol). Yellow crystals of **3** were obtained in 87% yield. Anal. Calcd for C<sub>24</sub>H<sub>17</sub>N<sub>4</sub>O<sub>4</sub>Cd: C, 53.60; H, 3.19; N, 10.42%. Found: C, 53.45; H, 3.16; N, 10.38%. IR (KBr pellet, cm<sup>-1</sup>): 1639 (w), 1606 (m), 1560 (s), 1501 (m), 1425 (w), 1392 (m), 1310 (w), 1109(w), 1070 (m), 970 (m), 841 (w), 717 (m).

**Preparation of [Cd(L)<sub>0.5</sub>(PBEA)]·H<sub>2</sub>O (**4**).** Complex **4** was prepared by the same procedure used for preparation of **3** except that H<sub>2</sub>DC (10.9 mg, 0.05 mmol) was replaced by H<sub>2</sub>PBEA (9.7 mg, 0.05 mmol). Colorless crystals of **4** were obtained in 60% yield. Anal. Calcd for C<sub>22</sub>H<sub>19</sub>N<sub>4</sub>O<sub>5</sub>Cd: C, 49.69; H, 3.60; N, 10.53%. Found: C,

49.57; H, 3.54; N, 10.48%. IR (KBr pellet, cm<sup>-1</sup>): 1608 (s), 1557 (s), 1511 (s), 1395 (s), 1288 (w), 1257 (m), 1112 (w), 1066 (m), 936 (m), 864 (w), 760 (w).

**Preparation of [Cd<sub>2</sub>(L)(MBEA)<sub>2</sub>]·4H<sub>2</sub>O (**5**).** Complex **5** was obtained by the same procedure used for preparation of **4** except that H<sub>2</sub>PBEA (9.7 mg, 0.05 mmol) was replaced by H<sub>2</sub>MBEA (9.7 mg, 0.05 mmol). Yellow block crystals of **5** were obtained in 80% yield. Anal. Calcd for C<sub>44</sub>H<sub>42</sub>N<sub>8</sub>O<sub>12</sub>Cd<sub>2</sub>: C, 48.06; H, 3.85; N, 10.19%. Found: C, 47.93; H, 3.83; N, 10.16%. IR (KBr pellet, cm<sup>-1</sup>): 1611 (s), 1565 (s), 1507 (s), 1389 (s), 1321 (m), 1274 (w), 1249 (w), 1114 (w), 1084 (m), 1009 (w), 926 (w), 864 (w), 765 (m), 719 (m).

**Preparation of [Zn(L)<sub>0.5</sub>(MBEA)]·2H<sub>2</sub>O (**6**).** Complex **6** was obtained by the same procedure used for preparation of **5** except that the metal salt was replaced by ZnSO<sub>4</sub>·7H<sub>2</sub>O (14.4 mg, 0.05 mmol). Yellow crystals of **6** were obtained in 86% yield. Anal. Calcd for C<sub>22</sub>H<sub>21</sub>N<sub>4</sub>O<sub>6</sub>Zn: C, 52.55; H, 4.21; N, 11.14%. Found: C, 52.42; H, 4.19; N, 11.11%. IR (KBr pellet, cm<sup>-1</sup>): 1639 (s), 1611 (s), 1580 (s), 1525 (m), 1507 (m), 1367 (s), 1321 (m), 1274 (w), 1122 (w), 1086 (m), 1073 (m), 1020 (w), 946 (w), 839 (w), 760 (w), 719 (m).

**Crystallography.** The crystallographic data collections for **1–6** were carried out on a Bruker Smart Apex CCD area detector diffractometer with graphite-monochromated Mo Kα radiation (λ = 0.71073 Å) at 20(2) °C using ω-scan technique. The diffraction data were integrated by using the SAINT program,<sup>22</sup> which was also used for the intensity corrections for the Lorentz and polarization effects. Semiempirical absorption corrections were applied using SADABS program.<sup>23</sup> The structures were solved by direct methods, and all of the non-hydrogen atoms were refined anisotropically on F<sup>2</sup> by the full-matrix least-squares technique using the SHELXL-97 crystallographic software package.<sup>24</sup> The hydrogen atoms except those of water molecules were generated geometrically and refined isotropically using the riding model. The hydrogen atoms of free water molecules in the complexes were not found. Atoms C2, C3, C4, C5, and C6 in **2** are disordered into two positions with site occupancies of 0.459(7) and 0.541(7), respectively. The C10, C11, C21, and C22 in **3** are disordered into two positions with site occupancies of 0.473(10) and 0.527(10), respectively, while the C24 and C25 also have two disordered positions with site occupancies of 0.490(6) and 0.510(6), respectively. Atoms O3 and O4 in **4** are also disordered into two positions, each with a site occupancy of 0.50. The details of the crystal parameters, data collection, and refinements for the complexes are summarized in Table 1, and selected bond lengths and angles are listed in Table 2.

## RESULTS AND DISCUSSION

**Crystal Structure of [Zn(L)<sub>0.5</sub>(CO<sub>3</sub>)]·H<sub>2</sub>O (**1**).** The results of single crystal X-ray diffraction analysis revealed that the asymmetric unit of **1** consists of half a molecule of [Zn(L)<sub>0.5</sub>(CO<sub>3</sub>)]·H<sub>2</sub>O, in which the Zn<sup>II</sup> atom is on the specific position with half occupancy. It is noteworthy that the auxiliary carboxylate ligand of H<sub>3</sub>BTB was not incorporated in **1**, and instead the carbonate anion was found in **1**. As shown in Figure 1a, the central Zn<sup>II</sup> atom is four-coordinated with distorted tetrahedral coordination geometry by two O atoms (O1, O2B) from two different CO<sub>3</sub><sup>2-</sup> anions and two N atoms (N2, N2G) from two different L ligands, with Zn1–O bond distances of 1.939(4) and 1.955(4) Å and Zn1–N one of 2.025 Å (Table 2). Each L ligand connects four Zn<sup>II</sup> atoms, and each CO<sub>3</sub><sup>2-</sup> anion adopts the μ<sub>2</sub>-η<sup>1</sup>:η<sup>1</sup>:η<sup>0</sup> coordination mode to link two Zn<sup>II</sup> atoms. If the connections of L ligands are ignored, the CO<sub>3</sub><sup>2-</sup> anions link the Zn<sup>II</sup> atoms to form an infinite one-dimensional (1D) chain, and then the chains are further linked together by L ligands to form a two-dimensional (2D) network (Figure 1b). And the 2D layers of **1** are packing in an -ABAB- sequence along the *a* axis (Figure 1c).

To further understand the structure of **1**, topological analysis by reducing multidimensional structure to simple node-and-linker net was performed. On the basis of the simplification

**Table 1. Crystal Data and Refinement Results for Complexes 1–6**

compound	1	2	3
empirical formula	C <sub>13</sub> H <sub>11</sub> N <sub>4</sub> O <sub>4</sub> Zn	C <sub>24</sub> H <sub>19</sub> N <sub>4</sub> O <sub>5</sub> Zn	C <sub>24</sub> H <sub>17</sub> N <sub>4</sub> O <sub>4</sub> Cd
formula weight	352.63	508.79	537.82
crystal system	orthorhombic	monoclinic	monoclinic
space group	<i>Pnmm</i>	<i>C2/c</i>	<i>C2/c</i>
<i>a</i> / Å	17.647(2)	20.742(3)	26.6249(10)
<i>b</i> / Å	5.2995(7)	19.431(3)	6.7018(3)
<i>c</i> / Å	13.9680(18)	12.3964(17)	23.2725(9)
$\beta$ / °	90.00	107.989(7)	105.0980(10)
<i>V</i> (Å <sup>3</sup> )	1306.3(3)	4752.0(12)	4009.3(3)
<i>Z</i>	4	8	8
<i>D<sub>c</sub></i> (g cm <sup>-3</sup> )	1.793	1.420	1.782
$\mu$ (mm <sup>-1</sup> )	1.906	1.075	1.132
<i>F</i> (000)	716	2080	2152
reflections collected	6017	11794	10836
independent reflections	1212	4206	3611
goodness-of-fit on <i>F</i> <sup>2</sup>	1.063	1.037	1.063
<i>R</i> <sub>1</sub> [ <i>I</i> > 2σ( <i>I</i> )] <sup>a</sup>	0.0385	0.0464	0.0279
<i>wR</i> <sub>2</sub> [ <i>I</i> > 2σ( <i>I</i> )] <sup>b</sup>	0.1128	0.1370	0.0763
compound	4	5	6
empirical formula	C <sub>22</sub> H <sub>19</sub> N <sub>4</sub> O <sub>5</sub> Cd	C <sub>44</sub> H <sub>42</sub> N <sub>8</sub> O <sub>12</sub> Cd <sub>2</sub>	C <sub>22</sub> H <sub>21</sub> N <sub>4</sub> O <sub>6</sub> Zn
formula weight	531.81	1099.59	502.80
crystal system	monoclinic	monoclinic	monoclinic
space group	<i>C2/c</i>	<i>C2/c</i>	<i>P2<sub>1</sub>/c</i>
<i>a</i> (Å)	10.997(3)	42.542(5)	6.761(5)
<i>b</i> (Å)	30.043(8)	13.6415(15)	16.856(5)
<i>c</i> (Å)	14.553(4)	15.2419(16)	18.782(5)
$\beta$ (°)	109.807(4)	99.301(2)	95.091(5)
<i>V</i> (Å <sup>3</sup> )	4523(2)	8729.1(16)	2132.0(18)
<i>Z</i>	8	8	4
<i>D<sub>c</sub></i> (g cm <sup>-3</sup> )	1.556	1.661	1.566
$\mu$ (mm <sup>-1</sup> )	1.005	1.048	1.201
<i>F</i> (000)	2120	4368	1036
reflections collected	11178	23791	11896
independent reflections	3956	8490	3782
goodness-of-fit on <i>F</i> <sup>2</sup>	1.084	1.128	1.035
<i>R</i> <sub>1</sub> [ <i>I</i> > 2σ( <i>I</i> )] <sup>a</sup>	0.0848	0.0607	0.0364
<i>wR</i> <sub>2</sub> [ <i>I</i> > 2σ( <i>I</i> )] <sup>b</sup>	0.2360	0.1787	0.1067

<sup>a</sup>*R*<sub>1</sub> =  $\sum ||F_o| - |F_c|| / \sum |F_o|$ . <sup>b</sup>*wR*<sub>2</sub> =  $|\sum w(|F_o|^2 - |F_c|^2)| / \sum w(F_o)^2$ , where  $w = 1/[\sigma^2(F_o^2) + (aP)^2 + bP]$ .  $P = (F_o^2 + 2F_c^2)/3$ .

principle,<sup>25</sup> each L ligand connects four Zn<sup>II</sup> atoms and each CO<sub>3</sub><sup>2-</sup> anion connects two Zn<sup>II</sup> atoms, while the Zn<sup>II</sup> atom links two L ligands and two CO<sub>3</sub><sup>2-</sup> anions; thus they can be regarded as a 4-, 2-, and 4-connector, respectively. Hence, the overall structure of **1** is a (4, 4)-connected binodal 2D net with stoichiometry of (4-c)(4-c)<sub>2</sub>, as shown in Figure 1d. The topological analysis by TOPOS program<sup>26</sup> suggests that the point (Schläfli) symbol of the net is (4.6<sup>4</sup>.8)<sub>2</sub>(4<sup>2</sup>.6<sup>4</sup>) and the topological type is 4,4L28.

**Crystal Structure of [Zn(L)<sub>0.5</sub>(DC)]·H<sub>2</sub>O (2).** When H<sub>2</sub>DC, instead of H<sub>3</sub>BTB, was used in the reaction, complex **2** was obtained. As shown in Figure 2a, each Zn<sup>II</sup> atom with distorted tetrahedral coordination geometry is surrounded by two N atoms (N1, N4) of imidazole groups provided by two L and

two O atoms (O2, O3) from two different DC<sup>2-</sup> ligands. The Zn–N bond lengths are 1.985(2) and 2.020(2) Å, and the ones of Zn–O are 1.939(2) and 1.943(2) Å, respectively. The bond angles around the Zn<sup>II</sup> atom are in the range of 96.5(1)–123.3(1)° (Table 2). There are two different kinds of DC<sup>2-</sup> ligands with the same μ<sub>2</sub>-bridge coordination mode (type I, Scheme 2), in which each carboxylate group is in μ<sub>1</sub>-η<sup>1</sup>:η<sup>0</sup>-monodentate fashion. Each L ligand connects four Zn<sup>II</sup> atoms using its four imidazole groups to give a 2D (4,4) net if the connections of the DC<sup>2-</sup> ligands are ignored (Figure 2b). Four Zn<sup>II</sup> atoms and four L ligands form a grid, with the Zn<sup>II</sup>–Zn<sup>II</sup> edge distances of 10.21 Å for Zn1A···Zn1B, 11.09 Å for Zn1B···Zn1C and Zn1D···Zn1A, 12.96 Å for Zn1C···Zn1D. The 2D layers are further linked together by one of the two DC<sup>2-</sup> ligands to form a 3-fold interpenetrating three-dimensional (3D) framework (Figure 2c). Interestingly, such 3-fold interpenetrating 3D net is connected by the other kinds of DC<sup>2-</sup> ligands to form the final self-interpenetrating 3D structure.

The topological analysis was carried out to get insight into the structure of **2**; each Zn<sup>II</sup> atom links two DC<sup>2-</sup> ligands and two L ligands, meanwhile each L and DC<sup>2-</sup> ligand connects four and two Zn<sup>II</sup> atoms, respectively. Thus, the Zn<sup>II</sup> atom and L ligand can be regarded as 4-connectors, and the DC<sup>2-</sup> ligand can be viewed as 2-connector. According to the simplification principle, the resulting structure of complex **2** is a (4, 4)-connected binodal 3D net with stoichiometry (4-c)(4-c)<sub>2</sub>, as shown in Figure 2d. Topological analysis by the TOPOS program<sup>23</sup> suggests that the point (Schläfli) symbol of the net is (6<sup>2</sup>.8<sup>4</sup>)(6<sup>4</sup>.8<sup>2</sup>)<sub>2</sub>, which is a new topology. As highlighted in Figure 2d, there are six-membered shortest circuits catenated to each other, which can be seen more clearly from Figure 2e. Thus, **2** is another example of the self-penetrating coordination polymer.<sup>27</sup>

**Crystal Structure of [Cd(L)<sub>0.5</sub>(DC)] (3).** Considering the structure of coordination polymers can be influenced by various factors including the metal centers,<sup>28</sup> we brought in another kind of d<sup>10</sup> metal center of Cd<sup>II</sup> and a new complex **3** was obtained. The asymmetric unit of **3** consists of one Cd<sup>II</sup> atom, half of L and one DC<sup>2-</sup> ligands. As illustrated in Figure 3a, Cd1 is six-coordinated with distorted octahedral coordination geometry by two N atoms (N12, N22E) from two different L ligands and four O atoms (O1B, O2, O3H, and O4H) from three different DC<sup>2-</sup>. The Cd1–O bond distances are in the range of 2.259(2)–2.497(3) Å, and the Cd1–N ones are 2.259(2) and 2.272(2) Å. The bond angles around the Cd<sup>II</sup> atom are in the range of 54.8(1)–167.3(1)° (Table 2).

The two carboxylate groups of each DC<sup>2-</sup> ligand in **3** exhibit two kinds of coordination modes which are different from those in **2**, one in a μ<sub>1</sub>-η<sup>1</sup>:η<sup>1</sup> chelating mode and the other one in a μ<sub>2</sub>-η<sup>1</sup>:η<sup>1</sup> bridging fashion (type II, Scheme 2); thus each DC<sup>2-</sup> ligand is a μ<sub>3</sub>-bridge. If the connections of L ligand are neglected, the DC<sup>2-</sup> ligands link Cd<sup>II</sup> atoms to form a 2D network (Figure 3b). Then four different layers are connected by L ligands to generate the final 3D framework structure of **3**, as illustrated in Figure 3c. Similar topological analysis was carried out to analyze the structure of **3**. As mentioned above, each DC<sup>2-</sup> and L ligand links three and four Cd<sup>II</sup> atoms, and accordingly the DC<sup>2-</sup> and L ligands can be viewed as 3- and 4-connected nodes, respectively. For each Cd<sup>II</sup> atom, it connects three DC<sup>2-</sup> ligands and two L ligands; hence, it can be treated as 5-connector. On the basis of the simplification principle, the overall structure of **3** is a (3,4,5)-connected trinodal net with stoichiometry (3-c)<sub>2</sub>(4-c)(5-c)<sub>2</sub>, as shown in Figure 3d.

Table 2. Selected Bond Distances (Å) and Angles (deg) for Complexes 1–6<sup>a</sup>

1				4			
Zn(1)–O(1)	1.939(4)	Zn(1)–O(2)#1	1.955(4)	N(22)#1–Cd(2)–O(1)	124.8(3)	N(22)–Cd(2)–O(2)	97.3(3)
Zn(1)–N(12)	2.025(3)			O(1)–Cd(2)–O(2)	52.1(3)	O(1)#1–Cd(2)–O(2)	131.8(3)
O(1)–Zn(1)–O(2)#1	106.0(2)	O(1)–Zn(1)–N(12)#2	105.8(1)	N(22)–Cd(2)–O(2)#1	79.8(3)	O(1)#1–Cd(2)–O(2)#1	52.1(3)
O(2)#1–Zn(1)–N(12)	108.7(1)	N(12)–Zn(1)–N(12)#2	120.8(2)	O(2)–Cd(2)–O(2)#1	175.8(4)		
2				5			
Zn(1)–O(3)	1.939(2)	Zn(1)–O(2)	1.943(2)	Cd(1)–N(32)#1	2.270(6)	Cd(1)–N(22)	2.270(6)
Zn(1)–N(1)	1.985(2)	Zn(1)–N(4)	2.020(2)	Cd(1)–O(3)	2.279(6)	Cd(1)–O(5)	2.351(5)
O(3)–Zn(1)–O(2)	96.5(1)	O(3)–Zn(1)–N(1)	118.3(1)	Cd(1)–O(6)#2	2.379(6)	Cd(1)–O(5)#2	2.475(6)
O(2)–Zn(1)–N(1)	123.3(1)	O(3)–Zn(1)–N(4)	104.3(1)	Cd(1)–O(4)	2.625(6)	Cd(2)–N(12)#3	2.265(6)
O(2)–Zn(1)–N(4)	112.6(1)	N(1)–Zn(1)–N(4)	101.0(1)	Cd(2)–N(42)	2.319(6)	Cd(2)–O(7)#4	2.332(5)
3				Cd(2)–O(1)#5	2.336(5)	Cd(2)–O(2)#3	2.350(6)
Cd(1)–O(3)#1	2.259(2)	Cd(1)–N(22)#2	2.272(2)	Cd(2)–O(1)#3	2.527(6)	Cd(2)–O(8)#4	2.542(5)
Cd(1)–O(1)#3	2.290(2)	Cd(1)–N(12)	2.298(2)	N(32)#1–Cd(1)–N(22)	172.1(2)	N(32)#1–Cd(1)–O(3)	94.8(2)
Cd(1)–O(2)	2.304(2)	Cd(1)–O(4)#1	2.497(3)	N(22)–Cd(1)–O(3)	87.8(3)	N(22)–Cd(1)–O(5)	86.8(2)
O(3)#1–Cd(1)–N(22)#2	112.4(1)	O(3)#1–Cd(1)–O(1)#3	83.13(8)	O(3)–Cd(1)–O(5)	140.5(2)	O(5)–Cd(1)–O(5)#2	75.2(2)
N(22)#2–Cd(1)–O(1)#3	96.73(7)	O(3)#1–Cd(1)–N(12)	145.9(1)	O(6)#2–Cd(1)–O(5)#2	52.2(2)	N(22)–Cd(1)–O(4)	85.6(2)
O(1)#3–Cd(1)–N(12)	96.5(1)	O(3)#1–Cd(1)–O(2)	84.24(8)	O(3)–Cd(1)–O(4)	52.6(2)	O(5)–Cd(1)–O(4)	88.0(2)
N(22)#2–Cd(1)–O(2)	98.42(8)	N(12)–Cd(1)–O(2)	87.74(9)	N(12)#3–Cd(2)–N(42)	171.8(2)	N(12)#3–Cd(2)–O(7)#4	94.1(2)
O(3)#1–Cd(1)–O(4)#1	54.8(1)	N(22)#2–Cd(1)–O(4)#1	167.3(1)	N(42)–Cd(2)–O(1)#5	86.7(2)	N(42)–Cd(2)–O(2)#3	94.9(3)
4				O(7)#4–Cd(2)–O(2)#3	91.9(2)	O(1)#5–Cd(2)–O(2)#3	120.3(2)
Cd(1)–O(3)	2.24(2)	Cd(1)–N(12)	2.285(7)	O(1)#5–Cd(2)–O(1)#3	69.9(2)	O(2)#3–Cd(2)–O(1)#3	50.4(2)
Cd(1)–O(3')	2.31(2)	Cd(1)–O(4')	2.34(2)	O(7)#4–Cd(2)–O(8)#4	53.5(2)	O(1)#5–Cd(2)–O(8)#4	94.7(2)
Cd(1)–O(4)	2.47(2)	Cd(2)–N(22)	2.270(6)				
Cd(2)–O(1)	2.274(7)	Cd(2)–O(2)	2.496(8)	6			
O(3)–Cd(1)–O(3)#1	82(1)	O(3)–Cd(1)–N(12)	117.6(6)	Zn(1)–O(1)	1.957(2)	Zn(1)–O(4)#1	1.980(2)
O(3)#1–Cd(1)–N(12)	125.7(5)	N(12)–Cd(1)–N(12)#1	92.5(4)	Zn(1)–N(12)	2.007(2)	Zn(1)–N(22)#2	2.033(2)
O(3)–Cd(1)–O(4')	36.1(7)	N(12)–Cd(1)–O(4')	145.9(6)	O(1)–Zn(1)–O(4)#1	104.94(9)	O(1)–Zn(1)–N(12)	122.04(9)
O(3)–Cd(1)–O(4)	53.8(6)	O(3)#1–Cd(1)–O(4)	126.7(6)	O(4)#1–Zn(1)–N(12)	114.95(8)	O(1)–Zn(1)–N(22)#2	116.10(9)
N(12)–Cd(1)–O(4)	102.1(5)	N(12)#1–Cd(1)–O(4)	77.4(4)	O(4)#1–Zn(1)–N(22)#2	95.73(8)	N(12)–Zn(1)–N(22)#2	100.29(9)
N(22)–Cd(2)–N(22)#1	94.6(4)	N(22)–Cd(2)–O(1)	114.6(3)				

<sup>a</sup>Symmetry transformations used to generate equivalent atoms: #1  $x, y + 1, z$ ; #2  $x, y, -z + 1$  for 1; #1  $x + 1/2, y + 1/2, z$ ; #2  $x, -y + 2, z - 1/2$ ; #3  $x, y + 1, z$  for 3; #1  $-x + 2, y, -z + 1/2$  for 4; #1  $x, y - 1, z$ ; #2  $-x, y, -z + 1/2$ ; #3  $x, y + 1, z$ ; #4  $-x, y + 1, -z + 1/2$ ; #5  $-x + 1/2, -y + 3/2, -z + 1$  for 5; #1  $x, -y + 1/2, z - 1/2$ ; #2  $-x + 1, y + 1/2, -z + 3/2$  for 6.

The point (Schläfli) symbol of the net is  $(4.6^3.8^6)_2(4^2.8^4)(6^3)_2$ , which is a new topology.

**Crystal Structure of  $[\text{Cd}(\text{L})_{0.5}(\text{PBEA})] \cdot \text{H}_2\text{O}$  (4).** When the flexible acid of  $\text{H}_2\text{PBEA}$ , instead of the semirigid one of  $\text{H}_2\text{DC}$ , was used in the reaction with the other experimental conditions unchanged as those for the synthesis of 3, complex 4 with different structure was obtained. As depicted in Figure 4a, there are two crystallographically different  $\text{Cd}^{\text{II}}$  atoms in the asymmetric unit of 4. The Cd1 is six-coordinated by four O atoms (O3, O4, O3A, and O4A) from two different  $\text{PBEA}^{2-}$ , and two N atoms (N12, N12A) from two different L ligands. The Cd1–N bond length is 2.285(7) Å and the Cd1–O ones are in the range of 2.24(2)–2.47(2) Å (Table 2). The Cd2 has a similar coordination environment with that of Cd1. Each Cd2 is also six-coordinated by four O atoms (O1, O2, O1A, and O2A) from two different  $\text{PBEA}^{2-}$  and two N atoms (N22, N22A) from two different L ligands. The Cd2–N bond length

is 2.270(6) Å and the Cd2–O ones are 2.274(7) and 2.496(8) Å (Table 2). The coordination angles around Cd2 extend from 52.1(3)–175.8(4)°, while the ones around Cd1 are in the range of 36.1(7)–145.9(6)° (Table 2). There are two different kinds of  $\text{PBEA}^{2-}$  ligands in 4 with the same coordination mode (type III, Scheme 2).

If the connections through the one kind of  $\text{PBEA}^{2-}$  are ignored, the L and another kind of  $\text{PBEA}^{2-}$  ligand links  $\text{Cd}^{\text{II}}$  atoms to form a 2D network in the  $ac$  plane as shown in Figure 4b. The adjacent 2D layers are connected by the above ignored  $\text{PBEA}^{2-}$  ligands along the  $b$  axis to give rise to the final 3D framework of 4 (Figure 4c). As described above, one L ligand connects four  $\text{Cd}^{\text{II}}$  atoms and each  $\text{Cd}^{\text{II}}$  atom links two L and two  $\text{PBEA}^{2-}$  ligands, while each of the  $\text{PBEA}^{2-}$  ligand joins two  $\text{Cd}^{\text{II}}$  atoms; thus L,  $\text{Cd}^{\text{II}}$ , and  $\text{PBEA}^{2-}$  can be treated as 4-, 4-, 2-connectors, respectively. According to the simplification rule, the resulting structure of 4 is a (4,4)-connected binodal

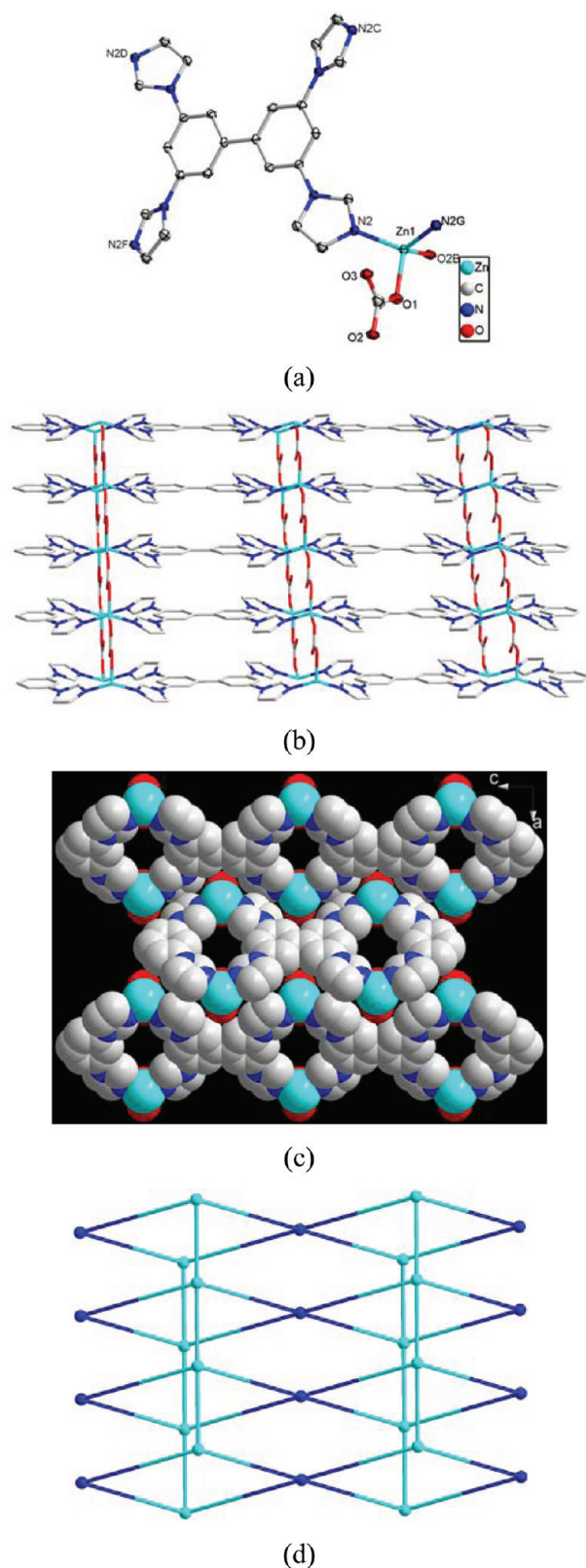


**Figure 1.** (a) The coordination environment of Zn<sup>II</sup> in **1** with the ellipsoids drawn at the 30% probability level. The hydrogen atoms and water molecule are omitted for clarity. Symmetry code: B  $x, 1 + y, z$ ; C  $-x, 2 - y, z$ ; D  $-x, 2 - y, -z$ ; F  $x, y, -z$ ; G  $x, y, 1 - z$ . (b) 2D layer structure of **1**. (c) The packing diagram of **1** along the *a* axis in an -ABAB- sequence. (d) Schematic representation of the (4,4)-connected binodal 2D network of **1** with  $(4.6^4.8)_2(4^2.6^4)$  topology (turquoise ball: Zn1; blue ball: the center of the L ligand).

net with the point (Schläfli) symbol of  $(4.6^4.8)_2(4^2.6^2.8^2)$ , which is a subnet of the *sta* net. It is noticed that there are large channels in **4** which can be seen clearly from the space-filling diagram (Figure 4d). Because of its large vacancy, it is apt to form an interpenetrating framework,<sup>29</sup> and accordingly, the final structure of **4** is a 3-fold interpenetrating framework as illustrated in Figure 4e.

**Crystal Structure of  $[\text{Cd}_2(\text{L})(\text{MBEA})_2] \cdot 4\text{H}_2\text{O}$  (**5**).** To further investigate the effect of carboxylate ligand on the structural diversity of the complexes,<sup>2d,30</sup> a flexible acid of H<sub>2</sub>MBEA, instead of the H<sub>2</sub>PBEA, was used in the preparation and complex **5** with different structure was successfully obtained. Figure 5a shows the coordination environments of two independent Cd<sup>II</sup> atoms with the atom numbering scheme. Cd1 atom is seven-coordinated with distorted pentagonal bipyramid coordination geometry by five O atoms (O3, O4, O5, O5D, and O6D) from three different MBEA<sup>2-</sup> and two N atoms (N22, N32A) from two different L ligands. It is notable that the Cd1–O4 distance of 2.625(6) Å is long indicating the weak interactions between them as observed in the previously reported Cd<sup>II</sup> complexes.<sup>31</sup> The Cd1–N bond lengths are both 2.270(6) Å and the Cd1–O ones are in the range of 2.279(6)–2.625(6) Å. The bond angles around Cd1 atom vary from 52.2(2) to 172.1(2)° (Table 2). The Cd2 has a similar coordination environment and geometry with Cd1. The Cd2–O bond lengths extend from 2.332(5) to 2.542(5) Å, and the Cd2–N bond lengths are 2.265(6) and 2.319(6) Å, respectively (Table 2). In the asymmetric unit of **5**, there are two different MBEA<sup>2-</sup> ligands with the same coordination mode (type IV, Scheme 2). One of the two carboxylate groups is chelating mode, and the other one is in  $\mu_2\text{-}\eta^2\text{-}\eta^1$  chelating/bridging mode in which the O1 and O5 atoms act as a bridge to connect two Cd<sup>II</sup> atoms (Cd2 and Cd2, Cd1 and Cd1) with Cd⋯Cd distances of 3.89 and 3.99 Å, respectively.

If the connections through the MBEA<sup>2-</sup> ligands are ignored, the L ligand links Cd<sup>II</sup> atoms using its imidazole groups to form an infinite hinged chain structure (Figure 5b). Then the adjacent chains are further connected by the MBEA<sup>2-</sup> ligands to generate a 2D network (Figure 5c). If the binuclear Cd<sub>2</sub>O<sub>2</sub> motif is viewed as the node, it links four L and two Cd<sub>2</sub>O<sub>2</sub> via four MBEA<sup>2-</sup> ligands, and thus it is treated as 6-connected node (Figure S1, Supporting Information). The L and MBEA<sup>2-</sup> ligands connect four Cd<sub>2</sub>O<sub>2</sub> and two Cd<sub>2</sub>O<sub>2</sub> motifs, and accordingly they can be regarded as 4- and 2-connected nodes, respectively. Thus the simplified overall structure of **5** is (4, 6)-connected binodal net with stoichiometry (4-c)(6-c), as shown in Figure 5d. The point (Schläfli) symbol for the net is  $(3^2.4^2.5^2)(3^4.4^4.5^4.6^3)$  calculated by the TOPOS program, and the topological type is 4,6L26.

**Crystal Structure of  $[\text{Zn}(\text{L})_{0.5}(\text{MBEA})] \cdot 2\text{H}_2\text{O}$  (**6**).** When ZnSO<sub>4</sub>·7H<sub>2</sub>O, instead of CdSO<sub>4</sub>·8/3H<sub>2</sub>O, was used in the synthesis under the same reaction conditions as those for the preparation of **5**, complex **6** was obtained. As illustrated in Figure 6a, the asymmetric unit of **6** consists of one Zn<sup>II</sup> atom, half of L, one MBEA<sup>2-</sup> ligand, and two free water molecules. The Zn<sup>II</sup> atom is four coordinated with distorted tetrahedral coordination geometry by two N atoms (N12, N22B) from two different L and two O atoms (O2, O4A) from two different MBEA<sup>2-</sup> ligands. The Zn–O bond lengths are 1.957(2) and 1.980(2) Å, and the ones of Zn–N are 2.007(2) and 2.033(2) Å. The bond angles around Zn<sup>II</sup> atom range from 95.73(8) to 122.04(9)° (Table 2). In **6**, the coordination mode of MBEA<sup>2-</sup> ligand is different from that in **5**, which is  $\mu_2$ -bridging fashion

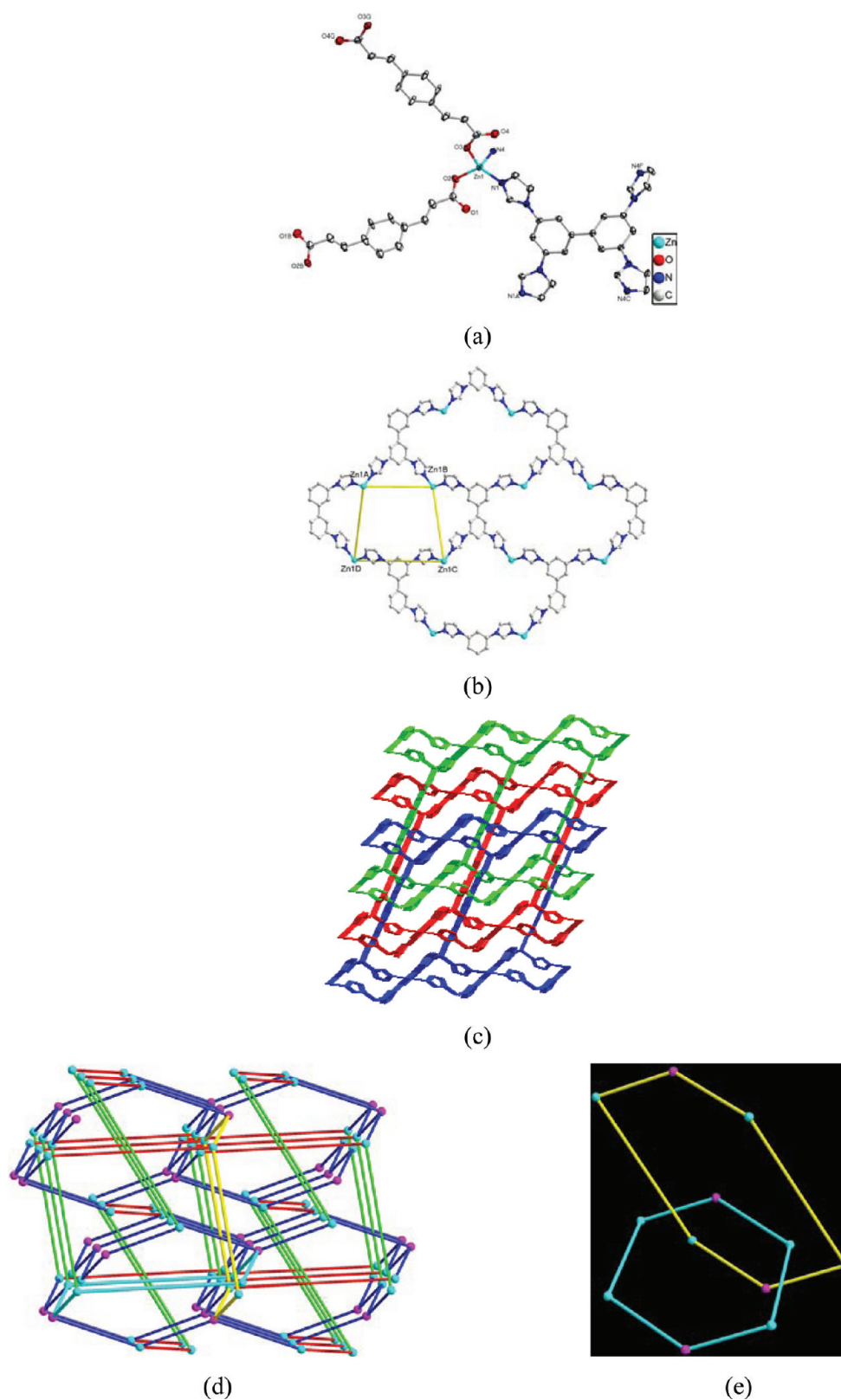
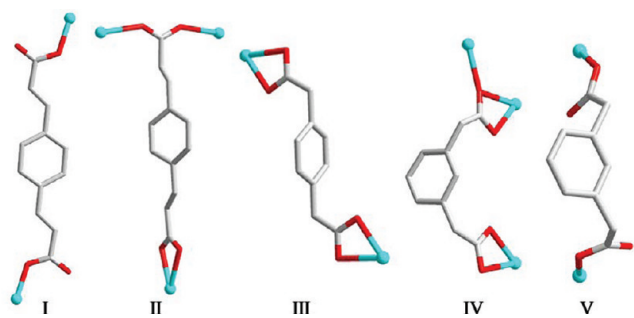


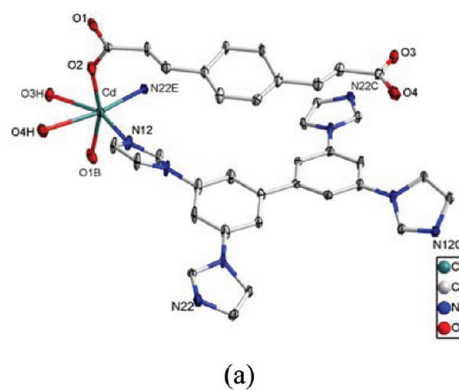
**Figure 2.** (a) Coordination environment of Zn<sup>II</sup> in **2** with the ellipsoids drawn at the 30% probability level. The hydrogen atoms and free water molecule are omitted for clarity. Symmetry code: A  $2 - x, y, 0.5 - z$ ; B  $2 - x, -y, 1 - z$ ; C  $0.5 + x, 0.5 + y, z$ ; F  $1.5 - x, 0.5 + y, 0.5 - z$ ; G  $1.5 - x, 0.5 - y, 2 - z$ . (b) 2D network of **2** constructed by Zn<sup>II</sup> atoms and L ligands. (c) The 3-fold interpenetrating 3D framework of **2** formed from 2D networks pillared by DC<sup>2-</sup> ligands. (d) Schematic representation of the (4, 4)-connected binodal self-penetrating 3D framework of **2** with two self-penetrated 6-membered shortest circuits highlighted (pink ball: the center of the L ligand; turquoise ball: Zn1; green stick: the normal DC<sup>2-</sup> ligand; red stick: the disordered DC<sup>2-</sup> ligand). (e) View of the self-penetration of two 6-membered circuits in **2**.

**Scheme 2. Coordination Modes of Multicarboxylate Ligands in Complexes 2–6**

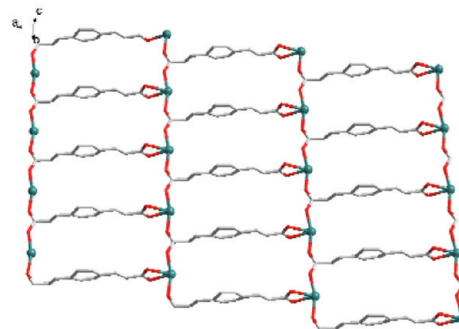


with each carboxylate group in  $\mu_1\text{-}\eta^1\text{:}\eta^0$ -monodentate mode (type V, Scheme 2). Each L ligand links four  $\text{Zn}^{\text{II}}$  atoms to generate an infinite 2D network (Figure 6b). Then the adjacent layers are further linked together by  $\text{MBEA}^{2-}$  ligands to form a 3D architecture (Figure 6c). From a topological view, each 2-connected bridging  $\text{MBEA}^{2-}$  ligand can be regarded as a linear linker. Each L ligand connects four  $\text{Zn}^{\text{II}}$  atoms and can be treated as a 4-connector. Each  $\text{Zn}^{\text{II}}$  atom can be regarded as 4-connected node since it links two L and two  $\text{MBEA}^{2-}$  ligands. Therefore, the overall structure of **6** is a 4-connected uninodal 3D net with stoichiometry  $(4\text{-c})(4\text{-c})_2$ , as shown in Figure 6d. The point (Schläfli) symbol for the net is  $(6^4)(8^2)$  calculated by the *TOPOS* program,<sup>25</sup> which has been referred by O’Keeffe and Wells to the *nbo* notation.<sup>26</sup>

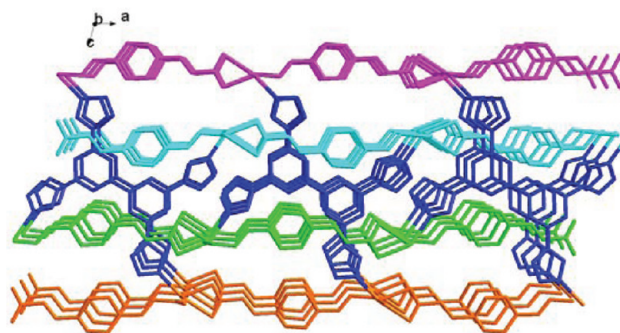
**Comparison the Structures of the Complexes 1–6.** Six new  $\text{Zn}^{\text{II}}/\text{Cd}^{\text{II}}$  complexes were successfully synthesized by using L and multidentate carboxylate ligands. And among these complexes, the auxiliary carboxylate ligands are completely deprotonated, which was confirmed by the IR spectral data (see Experimental Section) as well as the crystal structures as described above. It is known that multicarboxylate ligands are good candidates for the construction of MOFs with specific structure and topology due to their varied coordination modes. The different structures and topologies of the complexes **1**, **2**, and **6** with the same metal center of  $\text{Zn}^{\text{II}}$  and L ligand as well as **3**, **4**, and **5** with the same  $\text{Cd}^{\text{II}}$  and L ligand indicate that the multicarboxylate ligands have great influence on the structures of the complexes due to their different structures, flexibility, and coordination modes (Scheme 2). The auxiliary ligands except for  $\text{H}_3\text{BTB}$  used for preparation of **1** participate in the formation of the complexes. The dicarboxylate groups of  $\text{DC}^{2-}$ ,  $\text{PBEA}^{2-}$ ,  $\text{MBEA}^{2-}$  in **2–6** act as  $\mu_2$ ,  $\mu_3$ ,  $\mu_2$ ,  $\mu_3$ , and  $\mu_2$ -bridging ligands. And the carboxylate groups present different coordination modes in **2–6**, namely,  $\mu_1\text{-}\eta^1\text{:}\eta^0$ -monodentate in **2**,  $\mu_1\text{-}\eta^1\text{:}\eta^1$ -chelate and  $\mu_2\text{-}\eta^1\text{:}\eta^1$ -bridge in **3**,  $\mu_1\text{-}\eta^1\text{:}\eta^1$ -chelate in **4**,  $\mu_1\text{-}\eta^1\text{:}\eta^1$ -chelate and  $\mu_2\text{-}\eta^2\text{:}\eta^1$ -chelate/bridge in **5**, and  $\mu_1\text{-}\eta^1\text{:}\eta^0$ -monodentate in **6**. In addition, complexes **1–6** show 2D and 3D structures with different topologies. In brief, the different modes of the carboxylate groups lead to the formation of the complexes with varied structures, and at the same time, make it difficult to predict the structures of the resulting complexes. On the other hand, during the syntheses of complexes **2** and **3** as well as **5** and **6**, the same auxiliary ligands and L ligand were used. However the obtained structures are distinct, which could be ascribed to the different nature of the metal ions such as ion radius, coordination number, and geometry. In **2**, each  $\text{Zn}^{\text{II}}$  atom is four-coordinated, while in **3** each  $\text{Cd}^{\text{II}}$  atom is six-coordinated. Similarly, in **5**, the  $\text{Cd}^{\text{II}}$  atoms are seven-coordinated, while in **6** each  $\text{Zn}^{\text{II}}$  is four-coordinated.



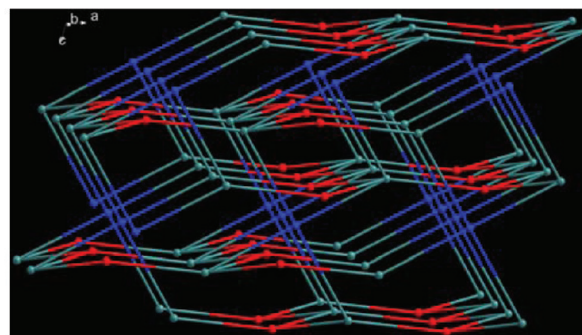
(a)



(b)



(c)



(d)

**Figure 3.** (a) Coordination environment of  $\text{Cd}^{\text{II}}$  in **3** with the ellipsoids drawn at the 30% probability level. The hydrogen atoms are omitted for clarity. Symmetry code: B  $x, 1 + y, z$ ; C  $1 - x, y, 1.5 - z$ ; E  $x, 2 - y, -0.5 + z$ ; H  $0.5 + x, 0.5 + y, z$ . (b) The layer structure of **3** constructed by  $\text{Cd}^{\text{II}}$  atoms and  $\text{DC}^{2-}$  ligands. (c) 3D framework of **3**: blue represented the L ligands, and the rest colors for different 2D layers. (d) Schematic representation of the 3D net of **3** with  $(4.6^3.8^6)_2(4^2.8^4)(6^3)_2$  topology (teal:  $\text{Cd}^{\text{II}}$  atom; red: the center of  $\text{DC}^{2-}$ ; blue: the center of L).

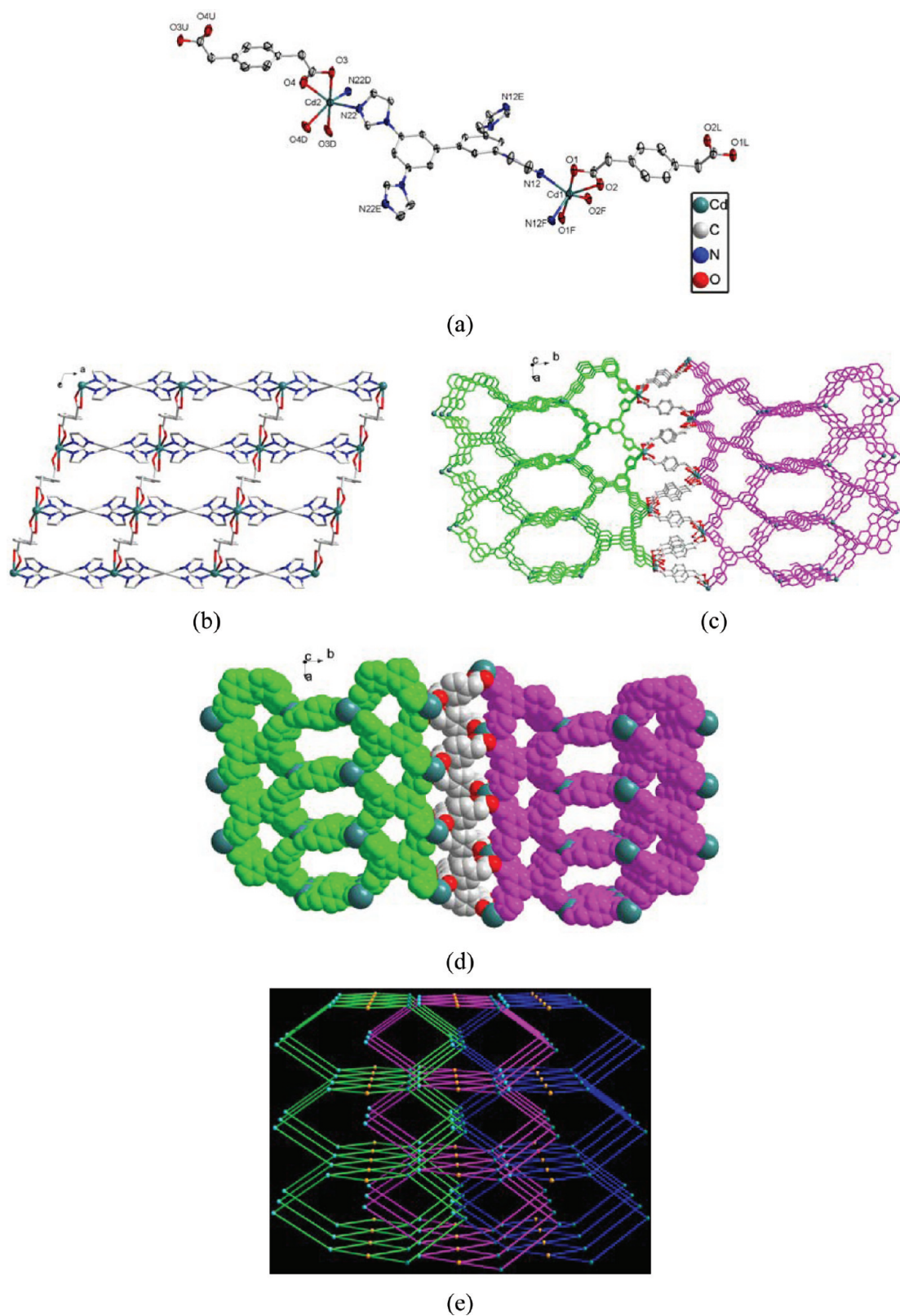


**Figure 4.** (a) Coordination environment of Cd<sup>II</sup> atoms in 4 with the ellipsoids drawn at the 30% probability level. The hydrogen atoms and free water molecules are omitted for clarity. Symmetry code: A  $2 - x, y, 0.5 - z$ ; B  $2 - x, 1 - y, 1 - z$ ; C  $1 - x, y, 0.5 - z$ ; D  $1.5 - x, -0.5 - y, -z$ . (b) 2D layer structure of 4 constructed by Cd<sup>II</sup> atoms, PBEA<sup>2-</sup> and L ligands in the *ac* plane. (c) 3D framework of 4: different colors for different layers. (d) The space-filling diagram of 4. (e) Schematic representation of the (4, 4)-connected binodal 3D 3-fold interpenetrating *sta* net of 4 with  $(4.6^4.8)_2(4^2.6^2.8^2)$  topology (yellow ball: the center of L ligand; teal ball: Cd<sub>2</sub>; turquoise ball: Cd<sub>1</sub>; different colors stick: independent 3D net).

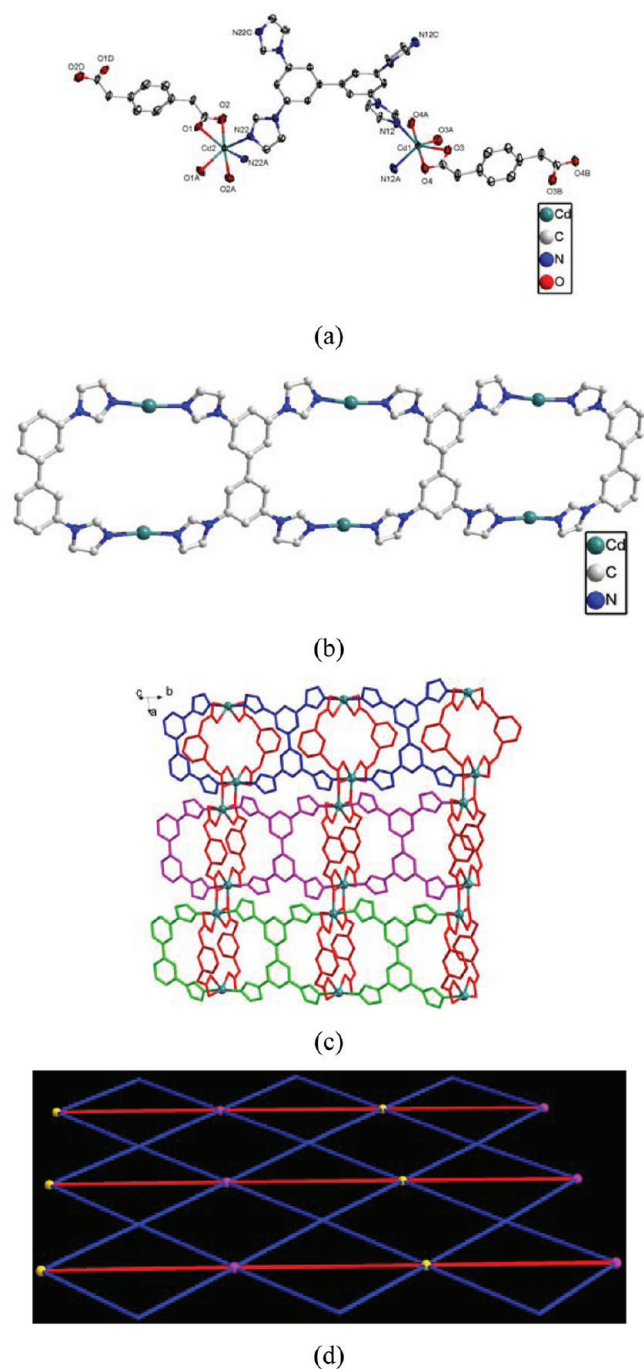


**Figure 5.** (a) Coordination environment of Cd<sup>II</sup> in **5** with the ellipsoids drawn at the 30% probability level. The hydrogen atoms and free water molecules are omitted for clarity. Symmetry code: A  $x, -1 + y, z$ ; B  $x, 1 + y, z$ ; D  $-x, y, 0.5 - z$ ; E  $-x, 1 + y, 0.5 - z$ ; F  $0.5 - x, 1.5 - y, 1 - z$ . (b) Hinged chain structure of **5** constructed by Cd<sup>II</sup> atoms and L ligands. (c) 2D network of **5** formed from hinged chains linked by MBEA<sup>2-</sup> ligands (different colors for different chains and red for the MBEA<sup>2-</sup> ligands). (d) Schematic representation of the (4, 6)-connected binodal 2D network of **5** with  $(3^2, 4^2, 5^2)(3^4, 4^4, 5^4, 6^3)$  topology (balls: Cd<sub>2</sub>O<sub>2</sub> units; blue stick: L ligand; red stick: MBEA<sup>2-</sup> ligand).

The results of this work provide further evidence to confirm that the auxiliary carboxylate ligands are versatile in construction of MOFs.

**Thermal Stability and PXRD of the Complexes.** The thermogravimetric analyses (TGA) of **1–6** were carried out

under N<sub>2</sub> atmosphere to examine the thermal stability of the coordination polymers and the results are shown in Figure S2, Supporting Information. Complex **1** shows a weight loss of 5.28% before 215 °C corresponding to the release of free water molecules (calcd 5.10%), and the decomposition of the residue was observed at 425 °C. For **2**, a weight loss of 3.62% was observed in the temperature range of 40–180 °C, which corresponds to the liberation of the free water molecules (calcd 3.62%), and further weight loss was observed at about 396 °C, owing to the collapse of the framework of **2**. No obvious weight loss was found for **3** before the decomposition of the framework occurred at about 395 °C, which is in good agreement with the result of its crystal structure. Complex **4** shows the weight loss of 3.48% between 54 and 230 °C, which is attributed to the release of the free water molecules (calcd 3.38%); the residue begins to decompose at 415 °C. For **5** and **6**, weight losses of 6.32% and 7.08% were observed in the temperature range of ca. 40–180 °C, which correspond to the liberation of the free water molecules (calcd 6.55% for **5** and 7.16% for **6**), respectively, and further weight losses were observed at about 300 and 335 °C, respectively, owing to the collapse of the frameworks of **5** and **6**.

The pure phase of the synthesized complexes **1–6** was confirmed by powder X-ray diffraction (PXRD) measurements and the results are shown in Figure S3, Supporting Information. And each PXRD pattern of the as-synthesized sample is very consistent with the simulated one.

**Sorption Property.** The results of structural analyses show that there are water molecules in the complexes except **3** without solvent molecules. Thus further TGA and PXRD measurements were carried out to ascertain the thermal stability of the complexes for sorption property investigation, and it was found that the water molecules in **1** and **6** can be removed completely by heating to give dehydrated samples of **1'** and **6'**, respectively without destroying the structure (Figures S2b and S3, Supporting Information). For complex **1**, the PXRD pattern of the dehydrated sample **1'** is consistent with the one of the as-synthesized one. While in the case of complex **6**, the PXRD pattern of the dehydrated sample **6'** is different from that of the as-synthesized one. Fortunately, the PXRD pattern of the rehydrated sample matches well with the as-synthesized one, indicating that the water molecule can induce the transformation of the framework. As shown in Figure 7, the sorption curves of N<sub>2</sub> at 77 K for samples **1'** and **6'** suggest only surface adsorption.<sup>32</sup> However, the H<sub>2</sub>O vapor sorption of **1'** and **6'** was observed. The final values of 73.056 cm<sup>3</sup> g<sup>-1</sup> (60.34 mg g<sup>-1</sup>) for **1'** and 100.21 cm<sup>3</sup> g<sup>-1</sup> (80.56 mg g<sup>-1</sup>) for **6'** at  $P = 0.99$  atm correspond to 1.09 and 2.09 H<sub>2</sub>O molecules per formula unit for **1** and **6**, respectively, which are close to the one and two molecules in **1** and **6** indicated by crystallographic analysis. The large hysteresis and incomplete desorption imply the strong adsorbate–adsorbent interactions.<sup>33</sup>

**Photoluminescence Properties of the Complexes.** The inorganic–organic hybrid coordination polymers, especially with d<sup>10</sup> metal centers, have been well investigated for fluorescence properties owing to their ability to adjust the emission of the substances.<sup>34</sup> Therefore, we carried out an investigation on the luminescence properties of the complexes in view of their potential applications as photoactive materials. The photoluminescence properties of **1–6** ligands were studied in the solid state in the room temperature

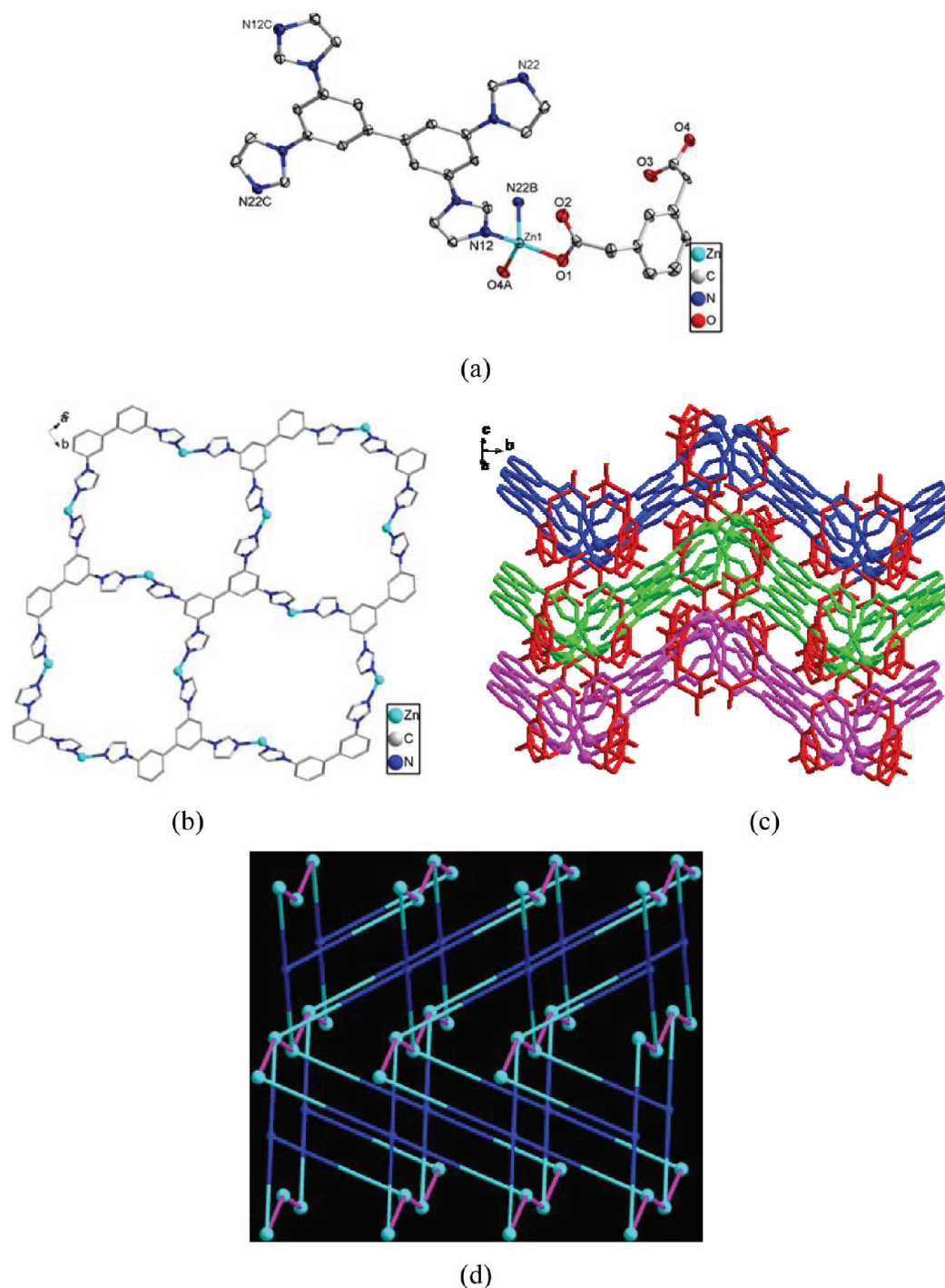


**Figure 6.** (a) Coordination environment of Zn<sup>II</sup> atom in **6** with the ellipsoids drawn at the 30% probability level. The hydrogen atoms and free water molecules are omitted for clarity. Symmetry code: A  $x, 0.5 - y, -0.5 + z$ ; B  $1 - x, 0.5 + y, 1.5 - z$ ; C  $-x, -y, 1 - z$ . (b) 2D layer structure of **6** constructed by Zn<sup>II</sup> atoms and L ligands. (c) 3D framework of **6** formed from layers connected by the MBEA<sup>2-</sup> ligands (different colors for different layers; red stick: the MBEA<sup>2-</sup> ligand). (d) Schematic representation of the 4-connected uninodal 3D nbo net of **6** with (6<sup>4</sup>)(8<sup>2</sup>) topology (turquoise ball: Zn1; blue ball: the center of the L ligand).

under the same experimental conditions, and the emission spectra are exhibited in Figure 8, while the emission spectra of the auxiliary ligands are given in Figure S4, Supporting Information. Intense emission bands were observed at 430 nm ( $\lambda_{\text{ex}} = 360$  nm) for L, 409 nm ( $\lambda_{\text{ex}} = 383$  nm) for H<sub>2</sub>DC, 454 nm ( $\lambda_{\text{ex}} = 365$  nm) for H<sub>2</sub>PBEA, and 434 nm ( $\lambda_{\text{ex}} = 375$  nm) for H<sub>2</sub>MBEA. Emission bands were observed at 433 nm ( $\lambda_{\text{ex}} = 353$  nm) for **1**, 437 nm ( $\lambda_{\text{ex}} = 373$  nm) for **2**, 454 nm

( $\lambda_{\text{ex}} = 380$  nm) for **3**, 417 nm ( $\lambda_{\text{ex}} = 330$  nm) for **4**, 427 nm ( $\lambda_{\text{ex}} = 355$  nm) for **5**, and 430 nm ( $\lambda_{\text{ex}} = 362$  nm) for **6**, respectively. Such photoluminescence emissions may be owing to the intraligand transition of the ligands as a result of their close similarity.<sup>35</sup> The red- or blue-shift of the emission maximum between the complex and the ligand was considered to originate from the influence of the coordination of the ligand to the metal centers.<sup>36</sup>

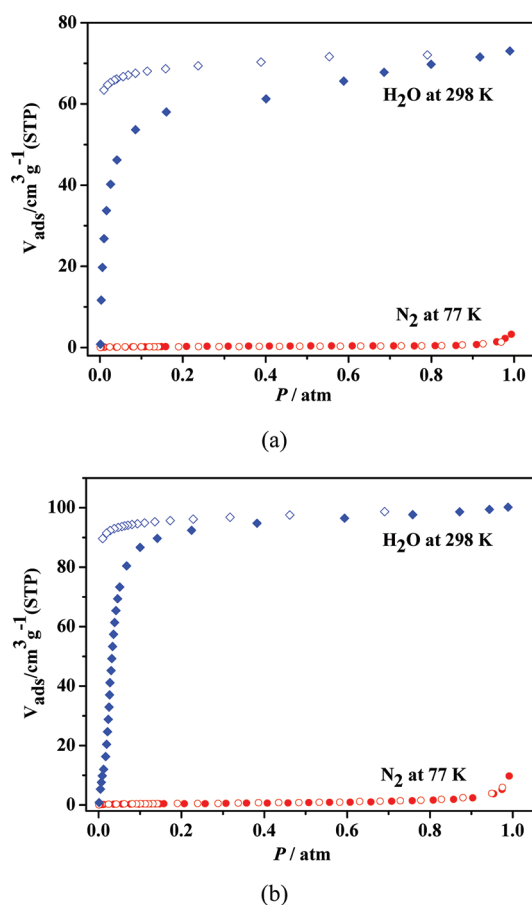


**Figure 7.**  $\text{N}_2$  and  $\text{H}_2\text{O}$  sorption isotherms at 77 and 298 K for **1** (a) and **6** (b): filled shape, adsorption; open shape, desorption.

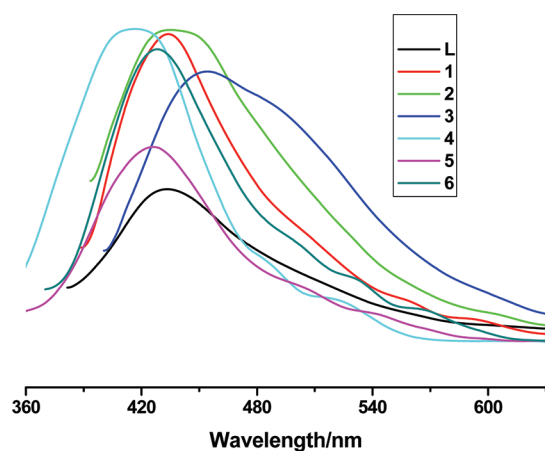


**Figure 8.** Emission spectra of **1–6** and **L** ligand in the solid state at room temperature.

## CONCLUSION

Six new coordination complexes with diverse structures and topologies were successfully constructed based on the rigid imidazole-containing ligand and varied auxiliary multicarboxylates with  $\text{Zn}^{\text{II}}$ / $\text{Cd}^{\text{II}}$  metal centers under hydrothermal conditions. The results showed that factors such as different flexibility, structure, coordination mode of the ligands, and the coordination number and geometry of the metal centers have remarkable impacts on the structure of the complexes. The

present study also demonstrates that the mixed ligands are powerful for construction of MOFs with diverse structures.

## ASSOCIATED CONTENT

### Supporting Information

X-ray crystallographic file in CIF format, 6-connected node (Figure S1), TGA (Figure S2), PXRD (Figure S3), emission of the auxiliary ligands (Figure S4). This information is available free of charge via the Internet at <http://pubs.acs.org>.

## AUTHOR INFORMATION

### Corresponding Author

\*Fax: 86 25 8331 4502. Tel: 86 25 8359 3485. E-mail: [sunwy@nju.edu.cn](mailto:sunwy@nju.edu.cn).

### Notes

The authors declare no competing financial interest.

## ACKNOWLEDGMENTS

This work was financially supported by the National Natural Science Foundation of China (Grant Nos. 91122001 and 21021062) and the National Basic Research Program of China (Grant No. 2010CB923303).

## REFERENCES

- (a) Lan, Y. Q.; Wang, X. L.; Li, S. L.; Su, Z. M.; Shao, K. Z.; Wang, E. B. *Chem. Commun.* **2007**, 4863. (b) Qi, Y.; Che, Y. X.; Zheng, J. M. *Cryst. Growth Des.* **2008**, *8*, 3602. (c) Carlucci, L.; Ciani, G.; Proserpio, D. M. *Coord. Chem. Rev.* **2003**, 247. (d) Bu, M. H.; Li, G. H.; Zou, Y. C.; Shi, Z.; Feng, S. H. *Inorg. Chem.* **2007**, *46*, 604. (e) Wang, X. L.; Qin, C.; Wang, E. B.; Su, Z. M. *Chem.—Eur. J.* **2006**, *12*, 2680. (f) Chen, S. -S.; Bai, Z. -S.; Fan, J.; Lv, G. -C.; Su, Z.; Chen, M. -S.; Sun, W. -Y. *CrystEngComm* **2010**, *12*, 3091.
- (a) Ma, S. Q.; Sun, D. F.; Ambrogio, M.; Fillinger, J. A.; Parkin, S.; Zhou, H. C. *J. Am. Chem. Soc.* **2007**, *129*, 1858. (b) Kesanli, B.; Cui, Y.; Smith, M. R.; Bittner, E. W.; Bockrath, B. C.; Lin, W. *Angew. Chem, Int. Ed.* **2005**, *44*, 72. (c) Dincă, M.; Dailly, A.; Tsay, C.; Long, J. R. *Inorg. Chem.* **2008**, *47*, 11. (d) Chen, S.-S.; Lv, G.-C.; Fan, J.; OKamura, T.; Chen, M.; Sun, W.-Y. *Cryst. Growth Des.* **2011**, *11*, 1082.
- (a) Duley, A.; Nethaji, M.; Ramanathan, G. *Cryst. Growth Des.* **2011**, *11*, 2238. (b) Jia, W. W.; Luo, J. H.; Zhu, M. L. *Cryst. Growth Des.* **2011**, *11*, 2386. (c) Ni, T. J.; Xing, F. F.; Shao, M.; Zhao, Y. M.; Zhu, S. R.; Li, M. X. *Cryst. Growth Des.* **2011**, *11*, 2999. (d) Sun, D.; Li, Y.-H.; Hao, H.-J.; Liu, F.-J.; Wen, Y.-M.; Huang, R.-B.; Zheng, L.-S. *Cryst. Growth Des.* **2011**, *11*, 3323.
- (a) Chen, K.; Liang, L.-L.; Zhang, Y.-Q.; Zhu, Q.-J.; Xue, S.-F.; Tao, Z. *Inorg. Chem.* **2011**, *50*, 7754. (b) Leeland, J. W.; White, F. J.; Love, J. B. *J. Am. Chem. Soc.* **2011**, *133*, 7320. (c) Hayashi, Y. *Coord. Chem. Rev.* **2011**, *255*, 2270. (d) Maruyama, M.; Guo, J.-D.; Nagase, S.; Nakamura, E.; Matsuo, Y. *J. Am. Chem. Soc.* **2011**, *133*, 6890.
- (a) Yamanoi, Y.; Sakamoto, Y.; Kusukawa, T.; Fujita, M.; Sakamoto, S.; Yamaguchi, K. *J. Am. Chem. Soc.* **2001**, *123*, 980. (b) Kima, D. J.; Mun, S.-D.; Yoon, S.; Oh, C. H.; Park, H.-R.; You, T.-S.; Lee, J.; Kima, Y. *Polyhedron* **2011**, *30*, 1076.
- (a) Jaremko, L.; Kirillov, A. M.; Smoleński, P.; Pombeiro, A. J. L. *Cryst. Growth Des.* **2009**, *9*, 3006. (b) Sarkar, M.; Biradha, K. *Chem. Commun.* **2005**, 2229. (c) Brizard, A.; Stuart, M.; Bommel, K. V.; Friggeri, A.; Jong, M. D.; Esch, J. V. *Angew. Chem., Int. Ed.* **2008**, *47*, 2063.
- (a) Luo, F.; Zheng, J. M.; Batten, S. R. *Chem. Commun.* **2007**, 3744. (b) Wen, G. L.; Wang, Y. Y.; Zhang, Y. N.; Yang, G. P.; Fu, A. Y.; Shi, Q. Z. *CrystEngComm* **2009**, *11*, 1519. (c) Zhang, J. P.; Kitagawa, S. *J. Am. Chem. Soc.* **2008**, *130*, 907.
- (a) Tan, H. Q.; Li, Y. G.; Zhang, Z. M.; Qin, C.; Wang, X. L.; Wang, E. B.; Su, Z. M. *J. Am. Chem. Soc.* **2007**, *129*, 10066. (b) Cheon, Y. E.; Suh, M. P. *Chem.—Eur. J.* **2008**, *14*, 3961. (c) Yan, L.; Yue, Q.; Jia, Q. X.; Lemerrier, G.; Gao, E. Q. *Cryst. Growth Des.* **2009**, *9*, 2984.

- (9) (a) Fan, J.; Hanson, B. E. *Inorg.chem.* **2005**, *44*, 6998. (b) Xu, G.-C.; Hua, Q.; Okamura, T.; Bai, Z.-S.; Ding, Y.-J.; Huang, Y.-Q.; Liu, G.-X.; Sun, W.-Y.; Ueyama, N. *CrystEngComm* **2009**, *11*, 261. (c) Hua, Q.; Zhao, Y.; Xu, G.-C.; Chen, M.-S.; Su, Z.; Cai, K.; Sun, W.-Y. *Cryst. Growth Des.* **2010**, *10*, 2553.
- (10) (a) Moorthy, J. N.; Natarajan, R.; Savitha, G.; Suchopar, A.; Richards, R. M. *J. Mol. Struct.* **2006**, *796*, 216. (b) Natarajan, R.; Savitha, G.; Moorthy, J. N. *Cryst. Growth Des.* **2005**, *5*, 69. (c) Natarajan, R.; Savitha, G.; Dominiak, P.; Wozniak, K.; Moorthy, J. N. *Angew. Chem., Int. Ed.* **2005**, *44*, 2115. (d) Moorthy, J. N.; Natarajan, R.; Savitha, G.; Venugopalan, P. *Cryst. Growth Des.* **2006**, *6*, 919.
- (11) Yamanoi, Y.; Sakamoto, Y.; Kusukawa, T.; Fujita, M.; Sakamoto, S.; Yamaguchi, K. *J. Am. Chem. Soc.* **2001**, *123*, 980.
- (12) (a) Rowsell, J. L. C.; Spencer, E. C.; Eckert, J.; Howard, J. A. K.; Yaghi, O. M. *Science* **2005**, *309*, 1350. (b) Tranchemontagne, D. J.; Ni, Z.; O'Keeffe, M.; Yaghi, O. M. *Angew. Chem., Int. Ed.* **2008**, *47*, 5136.
- (13) Wong-Foy, A. G.; Matzger, A. J.; Yaghi, O. M. *J. Am. Chem. Soc.* **2006**, *128*, 3494.
- (14) (a) Fang, Q.-R.; Zhu, G.-S.; Xue, M.; Zhang, Q.-L.; Sun, J.-Y.; Guo, X.-D.; Qiu, S.-L.; Xu, S.-T.; Wang, P.; Wang, D.-J.; Wei, Y. *Chem.—Eur. J.* **2006**, *12*, 3754. (b) Huang, K.-L.; Liu, X.; Li, J.-K.; Ding, Y.-W.; Chen, C.; Zhang, M.-X.; Xu, X.-B.; Song, X.-J. *Cryst. Growth Des.* **2010**, *10*, 1508.
- (15) (a) Babb, J. E. V.; Burrows, A. D.; Harrington, R. W.; Mahon, M. F. *Polyhedron* **2003**, *22*, 673. (b) Pan, L.; Adams, K. M.; Hernandez, H. E.; Wang, X. T.; Zheng, C.; Hattori, Y.; Kaneko, K. *J. Am. Chem. Soc.* **2003**, *125*, 3062.
- (16) Burrows, A. D.; Donovan, A. S.; Harrington, R. W.; Mahon, M. F. *Eur. J. Inorg. Chem.* **2004**, 4686.
- (17) (a) Hou, L.; Lin, Y. Y.; Chen, X. M. *Inorg. Chem.* **2008**, *47*, 1346. (b) Xue, M.; Ma, S. Q.; Jin, Z.; Schaffino, R. M.; Zhu, G. S.; Lobkovsky, E. B.; Qiu, S. L.; Chen, B. L. *Inorg. Chem.* **2008**, *47*, 6825.
- (18) Su, Z.; Fan, J.; Okamura, T.; Sun, W. Y.; Ueyama, N. *Cryst. Growth Des.* **2010**, *10*, 3515.
- (19) Su, Z.; Lv, G. C.; Fan, J.; Liu, G. X.; Sun, W. Y. *Inorg. Chem. Commun.* **2012**, *15*, 317.
- (20) (a) Liu, Y. W.; Meng, S. M.; Guo, Y.; Ren, S. B.; Tang, X. F. *Huaxue Yanjiu Yu Yingyong* **2002**, *14*, 79. (b) Malkov, A. V.; Vranková, K.; Sigerson, R. C.; Stončius, S.; Kočovský, P. *Tetrahedron* **2009**, *65*, 9481.
- (21) Wu, Q.; Hook, A.; Wang, S. *Angew. Chem., Int. Ed.* **2000**, *39*, 3933.
- (22) SAINT, Program for Data Extraction and Reduction; Bruker AXS, Inc.: Madison, WI, 2001.
- (23) Sheldrick, G. M. SADABS; University of Göttingen: Göttingen, Germany.
- (24) Sheldrick, G. M. SHELXS-97, Program for the Crystal Structure Solution; University of Göttingen: Göttingen, Germany, 1997.
- (25) (a) Blatov, V. A. *IUCr CompComm Newslett.* **2006**, *7*, 4. (b) Blatov, V. A. TOPOS, A Multipurpose Crystallochemical Analysis with the Program Package; Samara State University: Russia, 2009.
- (26) (a) O'Keeffe, M. see website: <http://rcsr.anu.edu.au/>. (b) Wells, A. F. *Three-Dimensional Nets and Polyhedral*; Wiley-Interscience: New York, 1977. (c) Wells, A. F. *Further Studies of Three-Dimensional Nets*; ACA Monograph 8; American Crystallographic Association: Pittsburgh, 1979; pp 661–663.
- (27) Blatov, V. A.; Carlucci, L.; Ciani, G.; Proserpio, D. M. *CrystEngComm* **2004**, *6*, 378.
- (28) (a) Ohi, H.; Tachi, Y.; Itoh, S. *Inorg. Chem.* **2004**, *43*, 4561. (b) Hennigar, T. L.; MacQuarrie, D. C.; Losier, P.; Rogers, R. D.; Zaworotko, M. J. *Angew. Chem., Int. Ed.* **1997**, *36*, 972. (c) Li, L. L.; Ya, Q. L.; Ma, J. F.; Yang, J.; Wei, G. H.; Zhang, L. P.; Su, Z. M. *Cryst. Growth Des.* **2008**, *8*, 2055.
- (29) (a) Ma, Y.; Cheng, A. L.; Zhang, J. Y.; Yue, Q.; Gao, E. Q. *Cryst. Growth Des.* **2009**, *9*, 867. (b) Yang, J.; Ma, J. F.; Liu, Y. Y.; Batten, S. R. *CrystEngComm* **2009**, *11*, 151. (c) Liang, X. Q.; Zhou, X. H.; Chen, C.; Xiao, H. P.; Li, Y. Z.; Zuo, J. L.; You, X. Z. *Cryst. Growth Des.* **2009**, *9*, 1041. (d) Carlucci, L.; Ciani, G.; Proserpio, D. M. *J. Chem. Soc., Dalton Trans.* **1999**, 1799. (e) Bradshaw, D.; Rosseinsky, M. J. *Solid State Sci.* **2005**, *7*, 1522.
- (30) (a) Yang, S. Y.; Long, L. S.; Jiang, Y. B.; Huang, R. B.; Zheng, L. S. *Chem. Mater.* **2002**, *14*, 3229. (b) Guo, X. D.; Zhu, G. S.; Li, Z. Y.; Sun, F. X.; Yang, Z. H.; Qiu, S. L. *Chem. Commun.* **2006**, 3172.
- (31) (a) Ouellette, W.; Hudson, B. S.; Zubieta, J. *Inorg. Chem.* **2007**, *46*, 4887. (b) Duan, X. Y.; Li, Y. Z.; Zang, S. Q.; Zhu, C. J.; Meng, Q. J. *CrystEngComm* **2007**, *9*, 758.
- (32) (a) Sing, K. S. W. *Pure Appl. Chem.* **1982**, *54*, 2201. (b) Choi, H.-S.; Suh, M. P. *Angew. Chem., Int. Ed.* **2009**, *48*, 6865.
- (33) Hou, C.; Liu, Q.; Lu, Y.; Okamura, T. -a.; Wang, P.; Chen, M.; Sun, W. -Y. *Microporous Mesoporous Mater.* **2012**, *152*, 96.
- (34) (a) Dong, Y. B.; Wang, P.; Huang, R. Q.; Smith, M. D. *Inorg. Chem.* **2004**, *43*, 4727. (b) Ciurtin, D. M.; Pschirer, N. G.; Smith, M. D.; Bunz, U. H. F.; zur Loye, H.-C. *Chem. Mater.* **2001**, *13*, 2743.
- (35) Huang, Y. Q.; Ding, B.; Song, H. B.; Zhao, B.; Ren, P.; Cheng, P.; Wang, H. G.; Liao, D. Z.; Yan, S. P. *Chem. Commun.* **2006**, 4906.
- (36) Su, Z.; Fan, J.; Chen, M.; Okamura, T.-a.; Sun, W.-Y. *Cryst. Growth Des.* **2011**, *11*, 1159.